# Contact Kinetics in Fractal Macromolecules

Maxim Dolgushev,[1] Thomas Guérin,[2] Alexander Blumen,[1] Olivier Bénichou,[3] and Raphaël Voituriez[3]
[1]*Physikalisches Institut, Universität Freiburg, Hermann-Herder-Strasse 3, 79104 Freiburg, Germany*
[2]*Université de Bordeaux and CNRS, Laboratoire Ondes et Matière d'Aquitaine (LOMA), UMR 5798, 33400 Talence, France*
[3]*Laboratoire de Physique Théorique de la Matière Condensée, CNRS/UPMC, 4 Place Jussieu, 75005 Paris, France*
(Received 21 May 2015; revised manuscript received 13 September 2015; published 9 November 2015)

We consider the kinetics of first contact between two monomers of the same macromolecule. Relying on a fractal description of the macromolecule, we develop an analytical method to compute the mean first contact time for various molecular sizes. In our theoretical description, the non-Markovian feature of monomer motion, arising from the interactions with the other monomers, is captured by accounting for the nonequilibrium conformations of the macromolecule at the very instant of first contact. This analysis reveals a simple scaling relation for the mean first contact time between two monomers, which involves only their equilibrium distance and the spectral dimension of the macromolecule, independently of its microscopic details. Our theoretical predictions are in excellent agreement with numerical stochastic simulations.

DOI: 10.1103/PhysRevLett.115.208301 PACS numbers: 82.35.Lr, 05.40.-a, 36.20.Ey, 82.20.Uv

*Introduction.*—Intramolecular reactions are ubiquitous in nature. Examples are provided by the formation of RNA hairpins [1] or DNA loops [2], the folding of polypeptides [3], as well as the appearance of cycles in synthetic polymers [4]. It is generally known that the structure of a macromolecule has a strong influence on the dynamics of its monomers [5,6], and that this complex intramolecular dynamics implies nontrivial reaction kinetics [7] in the diffusion limited regime. Until now, most of the theoretical work devoted to the reaction times in macromolecules has been limited mainly to linear chains [7–16]. However, there are numerous examples of macromolecules which differ from linear polymer chains [17,18]; their dynamic and static properties often suggest a fractal character [6,18,19]. In particular, the dynamics of fractal macromolecules is characterized by dynamical exponents that are different from those of linear chains [6,19–21], leading presumably to distinct first contact kinetics that cannot be deduced from existing works on linear chains. It is important to note the significance of fractals: They provide typical models, e.g., for hyperbranched polymers [6], proteins [21,22], sol-gel branched clusters [23], and colloidal aggregates [24].

The aim of this Letter is to propose a theoretical description of the mean first contact time (MFCT) between two monomers in a fractal macromolecule, described as a network of beads connected by springs. The cornerstone feature of such fractal models is the anomalous vibrational dynamics of the network [6,20,21]. It originates from the non-Debye density of states which is characterized through the so-called spectral dimension $d_s$ [25] (also known a "fracton" dimension [26]). In this Letter, we go beyond existing studies that focused on the specific case of linear chains only [7–16], and show on general grounds that $d_s$ (rather than the microscopic properties of the macromolecule) is the key parameter that controls intramolecular reaction kinetics. Indeed, the spectral dimension $d_s$ will be shown to leave its fingerprint in the scaling behavior of MFCTs with the equilibrium distance between monomers, as will be confirmed by explicit computations on examples of fractal structures (see Fig. 1).

It is important to stress that in the case of macromolecules, the interactions between monomers lead to an effective non-Markovian motion, which is the hallmark of monomer dynamics [27]. In this Letter, we take into account such non-Markovian features and describe the contact kinetics for fractal structures. We show explicitly that the non-Markovian effects increase with the complexity and the degree of branching of the macromolecules.

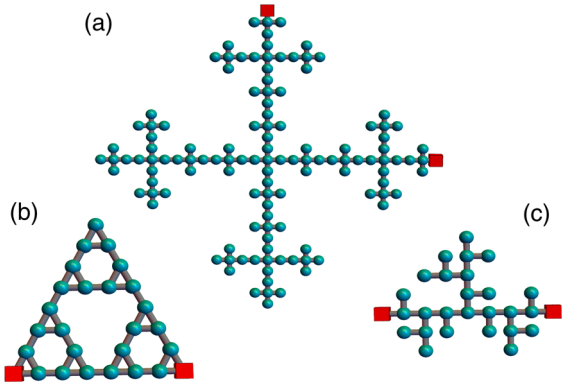


FIG. 1 (color online). Structure of fractal macromolecules investigated in this Letter. (a) Vicsek fractal, here of functionality (i.e., number of nearest neighbors of the branching sites) $f = 4$ (VF4); (b) dual Sierpiński gasket (DSG); (c) T fractal (TF). The reactive monomers for which we compute the MFCT are represented by red squares. These extended conformations show only the topology of the structures.

 

*Model.*—The macromolecular structures are represented by $N$ beads located at positions $\mathbf{r}_i(t)$ in a three-dimensional space and connected by springs of stiffness $K$. The free-draining dynamics of the structure is given by the Langevin equations [5,6]:

$$\zeta \frac{\partial}{\partial t}\mathbf{r}_i(t) + K\sum_{j=1}^{N} A_{ij}\mathbf{r}_j(t) = \mathbf{F}_i(t), \tag{1}$$

where $\mathbf{A} = (A_{kj})$ is the connectivity (Laplacian) matrix that describes the topology of the structure. The off-diagonal elements $A_{ij}$ are equal to $-1$ if beads $i$ and $j$ are connected, and 0 otherwise. For each bead $i$, the diagonal element $A_{ii}$ is equal to the number of bonds emanating from it. Also Eq. (1) includes friction forces $-\zeta\partial_t\mathbf{r}_i$ and stochastic forces $\mathbf{F}_i(t)$ obeying white noise statistics with amplitude $\langle F_{i\alpha}(t)F_{j\beta}(t')\rangle = 2k_BT\zeta\delta(t-t')\delta_{ij}\delta_{\alpha\beta}$, where $k_BT$ represents the thermal energy and $\alpha,\beta$ are spatial coordinates $x, y, z$. It is natural to introduce the monomeric relaxation time $\tau_0 = \zeta/K$, and the characteristic microscopic length $l = (3k_BT/K)^{1/2}$ (in the case of structures without loops $l^2$ is the mean-squared bond length).

Here we consider the contact kinetics between two given monomers denoted "reactive monomers," whose indexes are called $q_1$ and $q_2$ (see Fig. 1). We introduce the vector $\mathbf{R}(t)$ that joins them:

$$\mathbf{R}(t) \equiv \mathbf{r}_{q_1}(t) - \mathbf{r}_{q_2}(t) \equiv \sum_{i=1}^{N} h_i\mathbf{r}_i(t), \tag{2}$$

where $h$ is a $N$-dimensional vector defined by this equation, which has only two nonzero elements in positions $q_1$ and $q_2$. It is convenient to decompose the Gaussian vector $\mathbf{R}(t)$ as a sum of independent modes,

$$\mathbf{R}(t) = \sum_{\lambda} b_\lambda \mathbf{a}_\lambda(t), \tag{3}$$

where $\lambda$ represents all the distinct nonvanishing eigenvalues of $\mathbf{A}$, $b_\lambda^2$ is the norm of the orthogonal projection of the vector $h$ [defined in Eq. (2)] on the eigensubspace associated to $\lambda$ [28]. The $\mathbf{a}_\lambda(t)$ evolve independently of each other with the correlation function:

$$\langle a_{\lambda,\alpha}(t)a_{\lambda',\beta}(t')\rangle = l^2\delta_{\alpha,\beta}\delta_{\lambda,\lambda'}e^{-\lambda|t-t'|/\tau_0}/(3\lambda). \tag{4}$$

In this picture of independent modes, the normalized temporal autocorrelation function of the Cartesian components $(R_x(t), R_y(t), R_z(t))$ of vector $\mathbf{R}(t)$ follows from Eqs. (3) and (4):

$$\phi(t) \equiv \frac{\langle R_\alpha(t)R_\alpha(0)\rangle}{\langle R_\alpha(0)^2\rangle} = \left(\sum_\lambda \frac{b_\lambda^2}{\lambda}e^{-\lambda t/\tau_0}\right)\Big/\sum_\lambda \frac{b_\lambda^2}{\lambda}. \tag{5}$$

Since $\mathbf{R}(t)$ is a Gaussian stochastic process, it is entirely characterized by the function $\phi(t)$. We also introduce $n = \langle[\mathbf{R}(t)/l]^2\rangle = \sum_\lambda b_\lambda^2/\lambda$, which for macromolecules devoid of loops can be shown to be simply the number of bonds connecting the reactive monomers.

*Theories of first contact times.*—We now sketch briefly the method we use for the calculation of the MFCT, defined as the average time needed for the reactive monomers to be separated by a distance smaller than $a$ (called the capture radius), starting from an initial equilibrium configuration in which the reactive monomers are not in contact. We introduce the joint probability density $f(\{\mathbf{a}\}, t)$ that contact is made for the first time at time $t$ and that, at this first passage event, the macromolecule has a configuration described by the set of modes $\{\mathbf{a}\} = (\mathbf{a}_1, \mathbf{a}_2\ldots)$. Let us partition the trajectories that lead to a configuration $\{\mathbf{a}\}$ (in which the contact condition is satisfied) into two steps, the first step consisting in reaching the target for the first time at $t'$, and the second step consisting in reaching the final configuration $\{\mathbf{a}\}$ in a time $t-t'$. The mathematical formulation that corresponds to this decomposition of events is

$$p(\{\mathbf{a}\}, t) = \int_0^t dt' \int d\{\mathbf{a}'\} f(\{\mathbf{a}'\}, t')p(\{\mathbf{a}\}, t-t'|\{\mathbf{a}'\}), \tag{6}$$

where $p(\{\mathbf{a}\}, t|\{\mathbf{a}'\}\})$ is the probability of $\{\mathbf{a}\}$ at $t$ starting from $\{\mathbf{a}'\}$ at $t=0$ while $p(\{\mathbf{a}\}, t)$ is the probability of $\{\mathbf{a}\}$ at $t$ starting from the initial conditions. Although Eq. (6) is exact, it is in general very difficult to solve. A classical approximation, introduced by Wilemski and Fixman (WF) [8], assumes that $f(\{\mathbf{a}\}, t)$ is proportional to the equilibrium distribution of configurations that satisfy the constraint that a contact is formed. Introducing this approximation into Eq. (6), integrating over all configurations, and taking the long time limit lead to the estimate $T_{\mathrm{WF}}$ of the mean first contact time [15]

$$T_{\mathrm{WF}} = \int_0^\infty dt\left\{\frac{e^{-a^2\phi(t)^2/[2\psi(t)]}}{[1-\phi(t)^2]^{3/2}} - \frac{Z(a/\psi(t)^{1/2})}{Z(a\sqrt{3}/l\sqrt{n})}\right\}, \tag{7}$$

where $\psi(t) = nl^2[1-\phi(t)^2]/3$ is the mean-square displacement of $R_x(t)$ and $Z(y) = \int_y^\infty dx x^2 e^{-x^2/2}$. While this approximation takes into account some aspects of the complex dynamics of the macromolecule through the correlation function $\phi$, it neglects non-Markovian (NM) effects which can be quantitatively important. These NM effects can be described by considering the distribution of configuration at the first contact event $\pi(\{\mathbf{a}\}) = \int_0^\infty dt f(\{\mathbf{a}\}, t)$. The analytic expression for $\pi(\{\mathbf{a}\})$ is unknown; following the case of linear polymers [12], we assume that it is well approximated by a Gaussian distribution, which is therefore characterized by its first and second moments. Its first moments, denoted $m_\lambda$, are the

average mode amplitudes $\mathbf{a}_\lambda$ at the first contact instant $t^*$ [in the direction of the vector $\mathbf{R}(t^*)$], while the second moments can be approximated by their equilibrium values. Then, a precise estimate of the MFCT is obtained by integrating (6) over all contact configurations, leading to

$$T_{\mathrm{NM}} = \int_0^\infty dt \left\{ \frac{e^{-R_\pi(t)^2/[2\psi(t)]}}{[1-\phi(t)^2]^{3/2}} - \frac{Z(a/\psi(t)^{1/2})}{Z(a\sqrt{3}/l\sqrt{n})} \right\}. \quad (8)$$

The difference between this expression and Eq. (7) lies in the presence of the reactive trajectory $R_\pi(t)$, defined as the average of $\mathbf{R}$ at a time $t$ after the first contact $t^*$ in the direction of $\mathbf{R}(t^*)$, and thus reads $R_\pi(t) = \sum_\lambda b_\lambda m_\lambda e^{-\lambda t/\tau_0}$. The involved $m_\lambda$ are obtained from a set of self-consistent equations, see the Supplemental Material [28] for details.

*Cyclization for small capture radius.*—In the limit of $a \to 0$ (while keeping a fixed number of monomers), only the dynamics at small time scales matters, where $\psi(t) \simeq 4D_0 t$ with the local diffusion constant $D_0 = k_B T/\zeta$. Also, at short times, we can write $R_\pi(t) \simeq R_\pi(0) = a$. Introducing these approximations into Eqs. (7) and (8), we deduce that both the WF and the NM theories predict a MFCT which reads

$$T \simeq \tau_0 \pi^{1/2} n^{3/2} l/(2\sqrt{6}a) \quad (\text{for } a \to 0). \quad (9)$$

Thus, in this regime the MFCT is independent of the particular polymeric structure, and has the same expression as in the case of linear chains [12,15]. The convergence of both Eqs. (7) and (8) to the scaling form (9) for small capture radius is demonstrated in Fig. 2.

*Scaling for large n.*—When the size of the structure grows, Eq. (9) is not valid anymore and the MFCT reflects then the complex monomer dynamics, which becomes subdiffusive, $\langle [\mathbf{r}_q(t) - \mathbf{r}_q(0)]^2 \rangle \sim t^\gamma$, with $\gamma$ a subdiffusive exponent related to the spectral dimension $d_s$ of the structure, $\gamma = 1 - d_s/2$ for $d_s < 2$ [20,25,26,29]. We first present a simple qualitative argument to derive the behavior

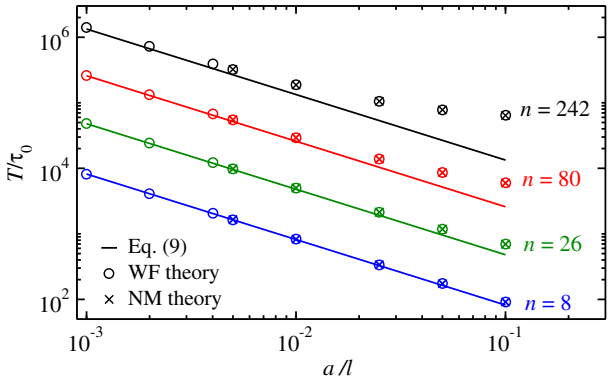


FIG. 2 (color online). $T_{\mathrm{NM}}$ [Eq. (8)] and $T_{\mathrm{WF}}$ [Eq. (7)] for Vicsek fractals of functionality $f = 4$ as a function of the capture radius $a$. The lines represent the results of Eq. (9).

of the MFCT as a function of $n$, which we explicitly check for the WF theory and validate next for the NM theory by a numerical analysis of the analytical results of Eq. (8).

For a Markovian subdiffusive walker whose subdiffusive exponent is $\gamma$, the time needed to find a pointlike target in a confining volume of size $L$ starting at a random position is proportional to $L^{2/\gamma}$ [35]. Given that in our case the typical length scale is $L \sim \sqrt{n}$, the scaling argument

$$T \sim \tau_0 n^{1/\gamma} \quad (10)$$

follows. We do not expect a strong dependence on the capture radius since the dynamics of a monomer is compact (or recurrent) [7,35]. In fact, the scaling (10) can be derived in the WF approximation by noting that for extremal monomers (i.e., monomers whose relative distance is maximal), the time $\tau_0 n^{1/\gamma}$ is also of the order of the maximal relaxation time $\tau_N$ [26,30], such that the correlation function scales as $\phi(t) = \tau_N \Phi(t/\tau_N)$. Once this equality is reported into Eq. (7) one obtains that $T \sim \tau_N$, which is the expected behavior (10), see the Supplemental Material [28] for details. Strikingly, the MFCT is found to depend on the polymer structure through $d_s$ only (and not on its microscopic details). In particular, this shows that the MFCT of highly branched structures ($\gamma \to 0$) differs significantly from that of linear chains ($\gamma = 1/2$).

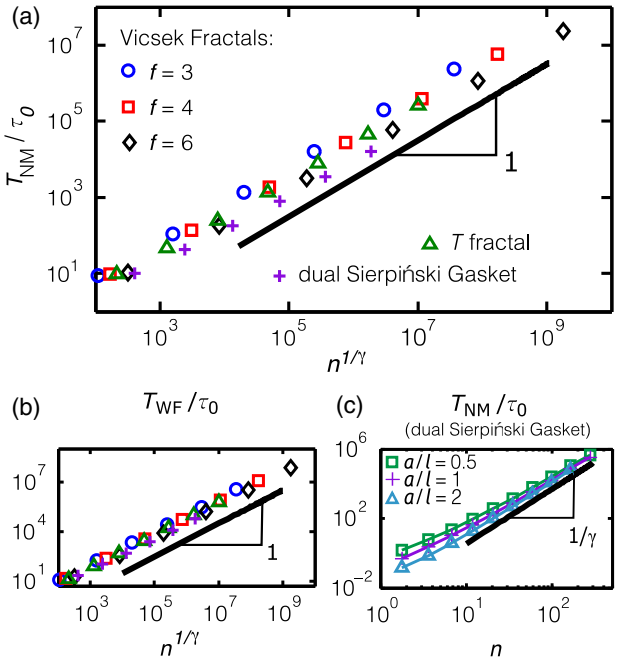


FIG. 3 (color online). (a) NM and (b) WF MFCT for different fractal structures as a function of $n^{1/\gamma}$. The parameter $\gamma$ is obtained from the known values [20,31,37] of the spectral dimension $d_s$: for Vicsek fractals of functionality $f$, $\gamma = \ln(3)/\ln(3f+3)$, for dual Sierpiński gasket $\gamma = \ln(5/3)/\ln(5)$, and for T fractal $\gamma = \ln(2)/\ln(6)$. The capture radius is $a = l$. (c) NM MFCT for the dual Sierpiński gasket for different values of $a$.

TABLE I. MFCT for the structures of Fig. 1 computed with the WF ($T_{\mathrm{WF}}$) and NM ($T_{\mathrm{NM}}$) theories [with Eqs. (7) and (8)], compared to the results $T_{\mathrm{simu}}$ of the stochastic simulations of (1). $1/\gamma$ indicates numerical values of the scaling exponent in (10) (in the case of linear chains it is equal to 2 [8,9,12]). All structures are of generation $g = 3$. The times are units of $\tau_0$.

| $a/l$ | Structure | $1/\gamma$ | $T_{\mathrm{WF}}$ | $T_{\mathrm{NM}}$ | $T_{\mathrm{simu}}$ |
|---|---|---|---|---|---|
| 1 | DSG | 3.15 | 3.85 | 2.38 | $2.41 \pm 0.02$ |
| | TF | 2.58 | 13.31 | 9.48 | $9.53 \pm 0.07$ |
| | VF3 | 2.26 | 166.8 | 111.5 | $113.6 \pm 0.9$ |
| | VF4 | 2.46 | 224.9 | 135.1 | $137.4 \pm 1.4$ |
| 2.5 | VF3 | 2.26 | 87.81 | 37.52 | $37.47 \pm 0.35$ |
| | VF4 | 2.46 | 128.3 | 47.1 | $45.3 \pm 0.5$ |

Now, checking the scaling (10) requires the actual computation of the correlation function $\phi(t)$, which itself involves the diagonalization of $\mathbf{A}$. However, a naive diagonalization of this matrix (as usually done for linear chains, where the analytic diagonalization is possible) does not allow us to deal with large enough structures. This difficulty can be overcome by exploiting the highly symmetric nature of the fractal macromolecules we are considering. First, we remark that the actual number of variables needed to be taken into account is the number of *distinct* eigenvalues, which is much lower than the total number of beads $N$. Then, one can set up a decimation procedure inspired by that used to find iterative formulas for the eigenvalues [20,36]. Adapting this decimation approach to the iterative computation of the coefficients $b_\lambda^2$ amounts to solving a linear algebra problem, as described in the Supplemental Material [28]. In practice, by using the WF and NM formalisms we were able to calculate the MFCT for macromolecules containing as many as 800 000 beads, which would not have been possible through direct diagonalization.

Based on the iterative computation of $b_\lambda^2$, we test the scaling behavior (Fig. 3) for different fractal structures (represented in Fig. 1) and therefore for several values of the subdiffusive exponent $\gamma$ (or $d_s$). As can be seen on Fig. 3, for all these structures, the scaling $T \sim n^{1/\gamma}$ is in good agreement with the predictions of both the NM theory and the WF theory. This confirms that the spectral dimension $d_s$ of the structure plays a fundamental role for MFCT. In particular, the functionality $f$, which determines $\gamma$, plays a crucial role and yields scaling behaviors that can differ significantly from those of linear chains. However, the presence of many loops in the dual Sierpiński gasket does not modify the scaling behavior of the MFCT: In Fig. 3(c) we show the results of the corresponding MFCT $T_{\mathrm{NM}}$ for three different values of $a$. We observe that all curves scale in the same way for large $n$, independently of the capture radius, a fact consistent with Eq. (10).

*Comparison with numerical simulations.*—We checked the validity of our theoretical predictions by performing Brownian dynamics simulations of Eq. (1), using the algorithm of Ref. [38] with fixed time steps. The results are presented in Table I for different fractal structures and capture radia $a$. We observe that the WF theory systematically overestimates the MFCT, whereas the NM theory describes the simulation data almost quantitatively, thereby validating the accuracy of our analysis.

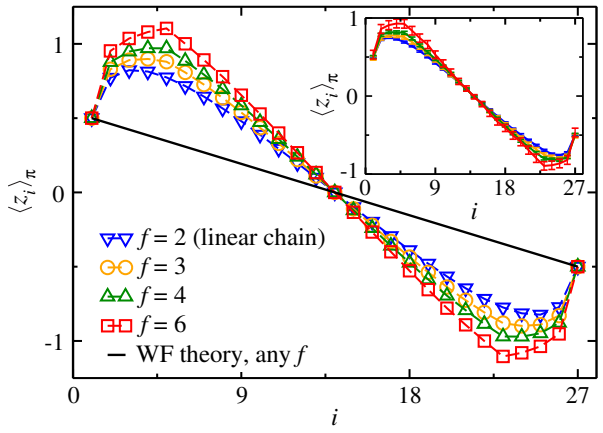


FIG. 4 (color online). Average spatial position $\langle z_i \rangle_\pi$ of the monomers (numbered through $i = 1, \ldots, n$) connecting reactants at the instant cyclization in the direction of the reaction, for Vicsek fractals of different functionalities $f$ with generation $g = 3$, as predicted by the NM (symbols) and WF theories (solid line). Inset: same quantity determined from simulations, with the same color code.

*Average conformations at first contact.*—Inspecting Fig. 3 reveals that the WF theory overestimates the MFCT by a numerical factor, which grows when $\gamma$ decreases. This fact is also clearly seen in Table I, and confirmed by the numerical simulations. This means that, with decreasing subdiffusive exponent $\gamma$, the macromolecular conformations at the instant of first contact differ more and more from equilibrium ones. To illustrate this fact, we present on Fig. 4 the average spatial positions of the monomers in Vicsek fractals at the instant of first contact $\langle z_i \rangle_\pi \equiv \langle \mathbf{r}_i(t^*) \cdot \hat{\mathbf{u}}(t^*) \rangle$, where $t^*$ represents the first contact instant, $\hat{\mathbf{u}}(t^*) = \mathbf{R}(t^*)/|\mathbf{R}(t^*)|$ gives the direction between the reactive monomers at $t^*$ and $i$ are the indices of the beads that lie between the reactive monomers (on the chain). In the equilibrium WF theory, all monomers between the reactants (on the chain) are on average also between the reactants in space at the instant of first contact, irrespectively of the functionality of the macromolecule. The NM theory, in turn, predicts that those monomers which are close to the reactants are in average outside the capture radius at $t^*$ (Fig. 4, symbols). Moreover, this effect is more pronounced for Vicsek fractals of higher functionalities, meaning that NM effects increase with the degree of hyperbranching of the macromolecule. As shown in the inset of Fig. 4, the simulations confirm these conclusions, although the value of $\langle z_i \rangle_\pi$ is slightly overestimated in the NM theory.

*Conclusion.*—Summarizing, we have studied the kinetics of first contact between two monomers belonging to the same fractal macromolecule. We identified two regimes: (i) for very small capture radius, the MFCT becomes independent of the macromolecular structure and originates essentially from the microscopic diffusive motion of the monomers, whereas (ii) for larger capture radius, the MFCT scales as a power law with the mean-square distance $n$ between the monomers, with an exponent related to the spectral dimension $d_s$ and independent of microscopic details. We confirmed this scaling law for a wide variety of structures (with and without loops). The non-Markovian effects are included by calculating the average equilibrium conformation of the whole macromolecule at the instant of first contact, and are found to be more important when the degree of hyperbranching of the structures increases. Finally, it would be interesting to explore how the MFCT varies with the location of the reactants in the structure or to generalize the theory to include the effect of hydrodynamic interactions, which typically would lead to new scalings [30].

M. D. and A. B. acknowledge the support of the DAAD through the PROCOPE program (Project No. 55853833), of the DFG through Grant No. Bl 142/11-1 and through IRTG Soft Matter Science (GRK 1642/1). T. G., O. B., and R. V. acknowledge the support of Campus France (Project No. 28252XE) and of the European Research Council starting Grant No. FPTOpt-277998.

[1] G. Bonnet, O. Krichevsky, and A. Libchaber, Proc. Natl. Acad. Sci. U.S.A. **95**, 8602 (1998); X. Wang and W. M. Nau, J. Am. Chem. Soc. **126**, 808 (2004).
[2] M. I. Wallace, L. Ying, S. Balasubramanian, and D. Klenerman, Proc. Natl. Acad. Sci. U.S.A. **98**, 5584 (2001); J.-F. Allemand, S. Cocco, N. Douarche, and G. Lia, Eur. Phys. J. E **19**, 293 (2006).
[3] L. J. Lapidus, W. A. Eaton, and J. Hofrichter, Proc. Natl. Acad. Sci. U.S.A. **97**, 7220 (2000); A. Möglich, K. Joder, and T. Kiefhaber, Proc. Natl. Acad. Sci. U.S.A. **103**, 12394 (2006).
[4] J. K. Gooden, M. L. Gross, A. Mueller, A. D. Stefanescu, and K. L. Wooley, J. Am. Chem. Soc. **120**, 10180 (1998); Y. Zheng, H. Cao, B. Newland, Y. Dong, A. Pandit, and W. Wang, J. Am. Chem. Soc. **133**, 13130 (2011); A. Burgath, A. Sunder, and H. Frey, Macromol. Chem. Phys. **201**, 782 (2000).
[5] M. Doi and S. F. Edwards, *The Theory of Polymer Dynamics* (Clarendon Press, Oxford, 1988).
[6] A. A. Gurtovenko and A. Blumen, Adv. Polym. Sci. **182**, 171 (2005).
[7] P.-G. De Gennes, J. Chem. Phys. **76**, 3316 (1982).
[8] G. Wilemski and M. Fixman, J. Chem. Phys. **60**, 866 (1974).
[9] A. Szabo, K. Schulten, and Z. Schulten, J. Chem. Phys. **72**, 4350 (1980).
[10] B. Friedman and B. O'Shaughnessy, Macromolecules **26**, 5726 (1993).
[11] I. M. Sokolov, Phys. Rev. Lett. **90**, 080601 (2003).
[12] T. Guérin, O. Bénichou, and R. Voituriez, Nat. Chem. **4**, 568 (2012).
[13] A. Amitai, I. Kupka, and D. Holcman, Phys. Rev. Lett. **109**, 108302 (2012).
[14] R. Afra and B. A. Todd, J. Chem. Phys. **138**, 174908 (2013).
[15] T. Guérin, O. Bénichou, and R. Voituriez, J. Chem. Phys. **138**, 094908 (2013); Phys. Rev. E **87**, 032601 (2013); T. Guérin, M. Dolgushev, O. Bénichou, R. Voituriez, and A. Blumen, Phys. Rev. E **90**, 052601 (2014); O. Bénichou, T. Guérin, and R. Voituriez, J. Phys. A **48**, 163001 (2015).
[16] J. Shin, A. G. Cherstvy, and R. Metzler, Soft Matter **11**, 472 (2015); ACS Macro Lett. **4**, 202 (2015).
[17] B. I. Voit and A. Lederer, Chem. Rev. **109**, 5924 (2009).
[18] W. Burchard, Adv. Polym. Sci. **143**, 113 (1999).
[19] I. M. Sokolov, J. Klafter, and A. Blumen, Phys. Today **55**, 48 (2002).
[20] A. Blumen, C. von Ferber, A. Jurjiu, and T. Koslowski, Macromolecules **37**, 638 (2004).
[21] S. Reuveni, R. Granek, and J. Klafter, Phys. Rev. Lett. **100**, 208101 (2008); Proc. Natl. Acad. Sci. U.S.A. **107**, 13696 (2010); S. Reuveni, J. Klafter, and R. Granek, Phys. Rev. Lett. **108**, 068101 (2012).
[22] R. Burioni, D. Cassi, F. Cecconi, and A. Vulpiani, Proteins **55**, 529 (2004); A. Banerji and I. Ghosh, Cell Mol. Life Sci. **68**, 2711 (2011).
[23] A. G. Zilman and R. Granek, Phys. Rev. E **58**, R2725 (1998).
[24] C. M. Sorensen, Aerosol Sci. Technol. **35**, 648 (2001).
[25] T. Nakayama, K. Yakubo, and R. L. Orbach, Rev. Mod. Phys. **66**, 381 (1994).
[26] S. Alexander and R. Orbach, J. Phys. Lett. **43**, 625 (1982).
[27] D. Panja, J. Stat. Mech. (2010) P06011; S. Gupta, A. Rosso, and C. Texier, Phys. Rev. Lett. **111**, 210601 (2013).
[28] See Supplemental Material at http://link.aps.org/supplemental/10.1103/PhysRevLett.115.208301 for the identification of $b_\lambda^2$ and the iterative calculation of correlation functions, as well as for the details of the MFCT theories, which includes Refs. [15,20,29–34].
[29] J.-U. Sommer and A. Blumen, J. Phys. A **28**, 6669 (1995).
[30] S. Reuveni, J. Klafter, and R. Granek, Phys. Rev. E **85**, 011906 (2012).
[31] M. G. Cosenza and R. Kapral, Phys. Rev. A **46**, 1850 (1992).
[32] C. D. Meyer, *Matrix Analysis and Applied Linear Algebra* (Siam, Philadelphia, 2000).
[33] F. Fürstenberg, M. Dolgushev, and A. Blumen, J. Chem. Phys. **138**, 034904 (2013).
[34] R. Rammal and G. Toulouse, J. Phys. Lett. **44**, 13 (1983).
[35] S. Condamin, O. Bénichou, V. Tejedor, R. Voituriez, and J. Klafter, Nature (London) **450**, 77 (2007).
[36] B. Meyer, E. Agliari, O. Bénichou, and R. Voituriez, Phys. Rev. E **85**, 026113 (2012).
[37] E. Agliari, Phys. Rev. E **77**, 011128 (2008).
[38] R. W. Pastor, R. Zwanzig, and A. Szabo, J. Chem. Phys. **105**, 3878 (1996).